Electronic Supplementary Information

Tuning slow magnetic relaxation behaviour in $\{Dy_2\}$-based one-dimensional chain via crystal field perturbation

Shui Yu,[a] Qinhua Zhang,[c] Huancheng Hu,*[,a] Zilu Chen,*[,a] Dongcheng Liu,[a] Yuning Liang[a] and Fupei Liang*[,a, b]

[a.] State Key Laboratory for Chemistry and Molecular Engineering of Medicinal Resources, School of Chemistry and Pharmaceutical Sciences, Guangxi Normal University, Guilin 541004, P. R. China. E-mail: zlchen@mailbox.gxnu.edu.cn; siniantongnian@126.com; fliangoffice@yahoo.com

[b.] Guangxi Key Laboratory of Electrochemical and Magnetochemical Functional Materials, College of Chemistry and Bioengineering, Guilin University of Technology, Guilin, 541004, P. R. China. E-mail: fliangoffice@yahoo.com

[c.] State Key Laboratory of Heavy Oil Processing, Institute of New Energy, College of Chemical Engineering, China University of Petroleum (East China), Qingdao 266580, P. R. China.

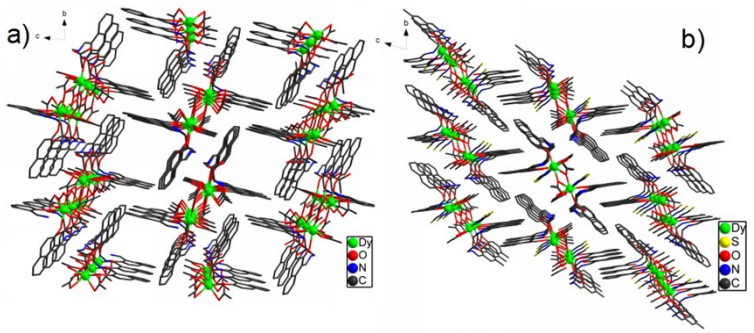

Fig. S1 The molecular packing structures of **1** (a) and **2** (b) viewed along the *a* axis (H atoms and solvent molecules are omitted for clarity).

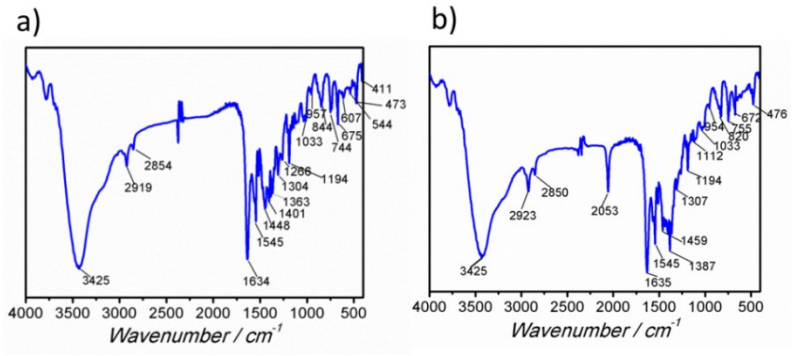

Fig. S2 FT-IR spectrum of **1** (a) and **2** (b).

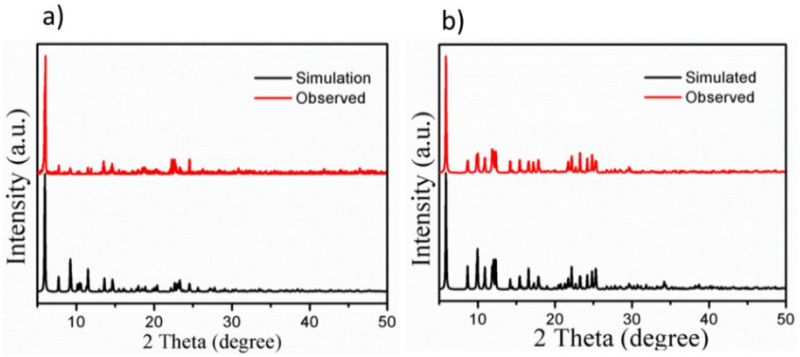

Fig. S3 PXRD patterns of **1** (a) and **2** (b).

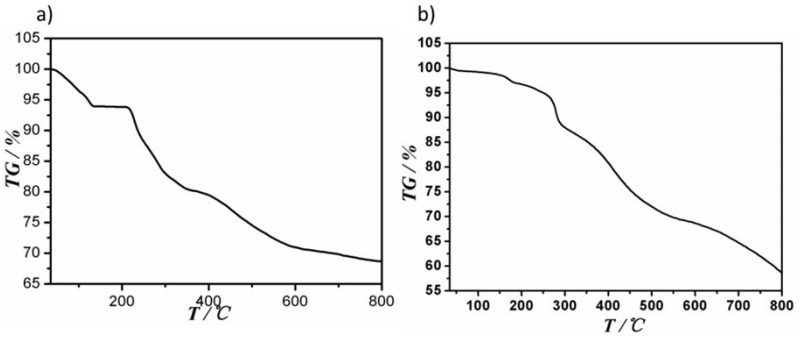

Fig. S4 The TGA curves for **1** (a) and **2** (b).

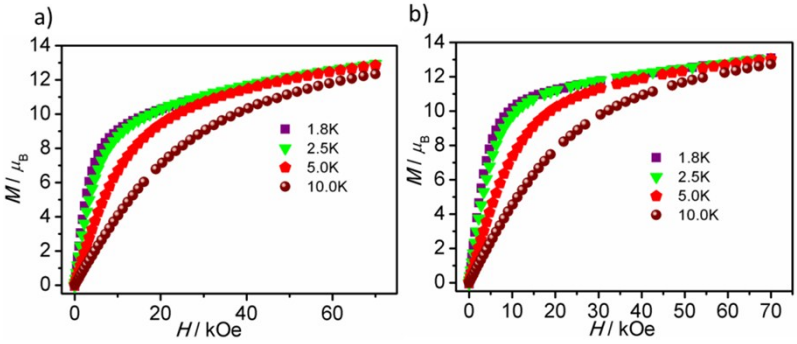

Fig. S5 *M* vs. *H* plots under different temperatures for **1** (a) and **2** (b).

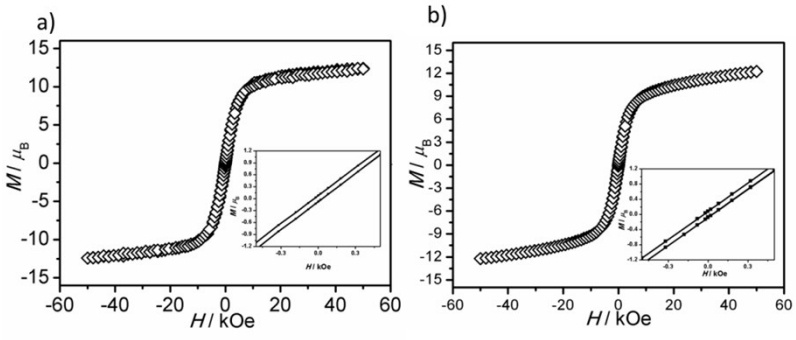

Fig. S6 Plots of magnetic hysteresis loops for **1** (a) and **2** (b).

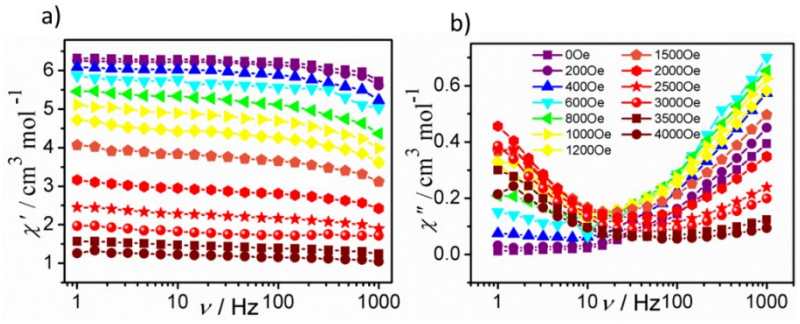

Fig. S7 Frequency-dependent in-phase (χ') and out-phase (χ'') ac susceptibilities under different dc fields at 2.0 K for **1**.

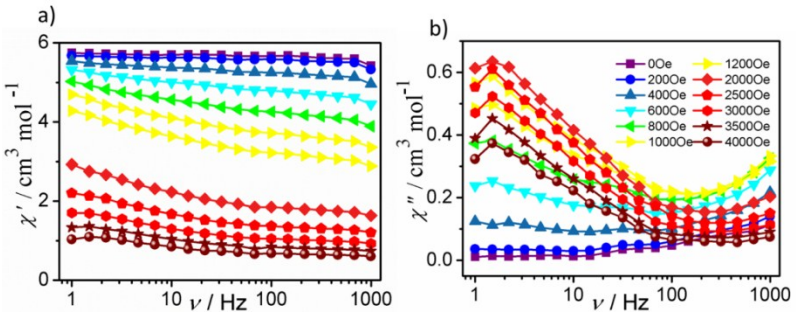

Fig. S8 Frequency-dependent in-phase (χ') and out-phase (χ'') ac susceptibilities under different dc fields at 2.0 K for **2**.

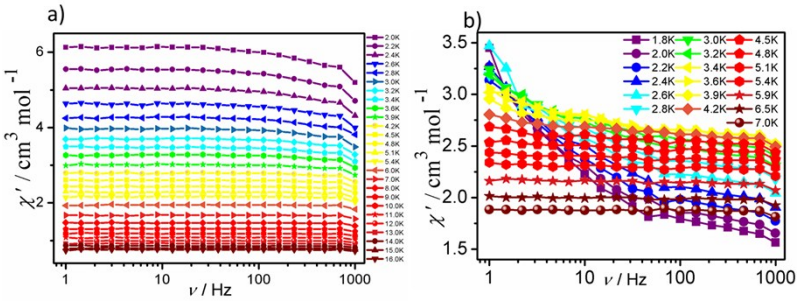

Fig. S9 Frequency-dependent in-phase (χ') ac susceptibilities for **1** (a) and **2** (b) under zero dc field.

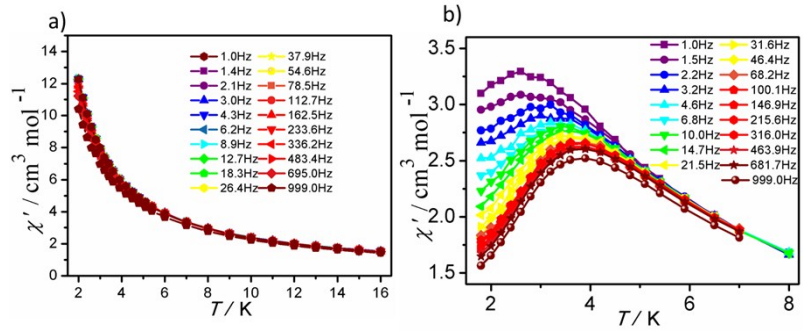

Fig. S10 Temperature dependence of the in-phase (χ') ac susceptibilities under 0 Oe in the

frequency range of 1-1000 Hz for **1** (a) and **2** (b).

Table S1. Crystallographic data of **1** and **2**.

Compound	**1**	**2**
Formula	$C_{64}H_{68}Dy_2N_4O_{20}$	$C_{62}H_{64}Dy_2N_6O_{16}S_2$
fw	1538.22	1538.31
T / K	293(2)	293(2)
λ / Å	0.71073	0.71073
Crystal system	triclinic	triclinic
Space group	$P\bar{1}$	$P\bar{1}$
a / Å	9.9272(2)	9.9101(6)
b / Å	11.8458(4)	11.7555(5)
c / Å	15.0341(4)	15.8011(5)
α / º	83.259(3)	73.569(3)
β / º	82.471(2)	88.693(4)
γ / º	76.012(2)	65.351(5)
V / Å^3	1693.97(8)	1595.15(12)
Z	1	1
D_c / g cm^{-3}	1.508	1.603
μ / mm^{-1}	2.261	2.461
F(000)	772.0	772.0
θ / °	3.34-25.000	3.27-25.000
Reflns collected	25041	22939
Reflns unique	5943	5598
R_{int}	0.0271	0.0535
GOF on F^2	1.105	1.066
R_1 [$I > 2\sigma(I)$]	0.0356	0.0459
wR_2 [$I > 2\sigma(I)$)]	0.1048	0.1351

R_1 (all data)	0.0369	0.0510
wR_2 (all data)	0.1068	0.1419

Table S2. Selected bond lengths and bond angles of **1**

Dy1-O1	2.304 (3)	Dy1-O3A	2.285 (2)	Dy1-O4	2.449 (3)
Dy1-O5	2.410 (3)	Dy1-O6	2.553 (3)	Dy1-O6B	2.349 (3)
Dy1-O7	2.452 (3)	Dy1-O8	2.510 (4)	Dy1-O9	2.566 (4)
O3B-Dy1-O1	87.00 (12)	O3B-Dy1-O4	86.37 (12)	O3B-Dy1-O5	78.63 (12)
O3B-Dy1-O6	124.66 (11)	O3B-Dy1-O6A	163.11 (12)	O3B-Dy1-O7	76.03 (11)
O3B-Dy1-O8	118.84 (10)	O3B-Dy1-O9	69.35 (12)	O5-Dy1-O1	125.53 (8)
O5-Dy1-O4	53.02 (11)	O5-Dy1-O7	76.94 (12)	O5-Dy1-O9	138.43 (12)
O6-Dy1-O1	147.40 (10)	O6-Dy1-O4	111.91 (11)	O6-Dy1-O5	74.00 (11)
O6-Dy1-O7	51.54 (10)	O6-Dy1-O9	102.96 (11)	O6A-Dy1-O1	85.74 (11)
O6A-Dy1-O4	76.98 (12)	O6A-Dy1-O5	93.26 (12)	O6A-Dy1-O7	116.88 (10)
O6A-Dy1-O9	123.97 (12)	O7-Dy1-O1	148.94 (12)	O7-Dy1-O4	129.42 (11)
O7-Dy1-O9	70.25 (12)	O8-Dy1-O1	86.77 (13)	O8-Dy1-O4	147.68 (13)
O8-Dy1-O5	145.67 (13)	O8-Dy1-O7	79.25 (13)	O8-Dy1-O9	49.70 (12)
O9-Dy1-O1	79.52 (12)	O9-Dy1-O4	144.78 (12)		

Symmetry codes: (A)1-X, 2-Y, 1-Z; (B) -1+X,+Y,+Z; (C) 1+X,+Y,+Z.

Table S3. Selected bond lengths and bond angles of **2**

Dy1-O1	2.290 (4)	Dy1-O3	2.270 (4)	Dy1-O4	2.354 (4)
Dy1-O4B	2.482 (4)	Dy1-O5B	2.501 (5)	Dy1-O6	2.422 (5)
Dy1-O7	2.423 (5)	Dy1-N3	2.378 (9)	O1-Dy1-O4	83.83 (15)
O1-Dy1-O4A	147.02 (15)	O1-Dy1-O5A	150.83 (16)	O1-Dy1-O6	125.31 (17)
O1-Dy1-O7	73.88 (16)	O1-Dy1-N3	85.0 (2)	O3B-Dy1-O1	84.03 (16)
O3B-Dy1-O4	165.86 (17)	O3B-Dy1-O4A	126.36 (16)	O3B-Dy1-O5A	75.11 (16)
O3A-Dy1-O6	84.51 (18)	O3A-Dy1-O7	89.41 (19)	O3B-Dy1-N3	97.0 (4)
O4-Dy1-O4A	67.24 (17)	O4-Dy1-O5A	118.77 (14)	O4-Dy1-O6	96.65 (17)
O4-Dy1-O7	80.27 (18)	O4-Dy1-N3	89.2(3)	O4A-Dy1-O5A	51.63 (14)

O6-Dy1-O4A	75.55 (16)	O6-Dy1-O5A	73.30 (17)	O7-Dy1-O4A	114.22 (16)
O7-Dy1-O5A	125.11 (16)	O7-Dy1-O6	52.71 (17)	N3-Dy1-O4A	79.3 (3)
N3-Dy1-O5A	77.7 (2)	N3-Dy1-O6	149.5 (2)	N3-Dy1-O7	157.2 (3)

Symmetry codes: (A) -1+X,+Y,+Z; (B) 2-X,1-Y,1-Z; (C) 1+X,+Y,+Z.

Table S4. SHAPE analysis of **1**

Configuration	ABOXIY
Enneagon (D_{9h})	32.533
Octagonal pyramid (C_{8v})	23.383
Heptagonal bipyramid (D_{7h})	15.822
Johnson triangular cupola J3 (C_{3v})	13.162
Capped cube J8 (C_{4v})	8.743
Spherical-relaxed capped cube (C_{4v})	7.790
Capped square antiprism J10 (C_{4v})	3.582
Spherical capped square antiprism (C_{4v})	2.886
Tricapped trigonal prism J51 (D_{3h})	3.712
Spherical tricapped trigonal prism (D_{3h})	3.288
Tridiminished icosahedron J63 (C_{3v})	10.615
Hula-hoop (C_{2v})	9.196
Muffin (C_s)	**2.817**

Table S5. SHAPE analysis of **2**

Configuration	ABOXIY
Octagon (D_{8h})	31.613
Heptagonal pyramid (C_{7v})	23.501
Hexagonal bipyramid (D_{6h})	13.320
Cube (O_h)	11.043
Square antiprism (D_{4d})	4.374
Triangular dodecahedron (D_{2d})	**3.308**
Johnson gyrobifastigium J26 (D_{2d})	11.008
Johnson elongated triangular bipyramid J14 (D_{3h})	27.405
Biaugmented trigonal prism J50 (C_{2v})	3.969
Biaugmented trigonal prism (C_{2v})	3.547
Snub diphenoid J84 (D_{2d})	4.249
Triakis tetrahedron (T_d)	11.870
Elongated trigonal bipyramid (D_{3h})	23.693